

Spatiotemporal chaos from bursting dynamics

Igal Berenstein and Yannick De Decker

Citation: *The Journal of Chemical Physics* **143**, 064105 (2015); doi: 10.1063/1.4927911

View online: <http://dx.doi.org/10.1063/1.4927911>

View Table of Contents: <http://scitation.aip.org/content/aip/journal/jcp/143/6?ver=pdfcov>

Published by the *AIP Publishing*

Articles you may be interested in

[Spatiotemporal chaos arising from standing waves in a reaction-diffusion system with cross-diffusion](#)

J. Chem. Phys. **136**, 034903 (2012); 10.1063/1.3676577

[Bifurcations in spiral tip dynamics induced by natural convection in the Belousov–Zhabotinsky reaction](#)

J. Chem. Phys. **130**, 024902 (2009); 10.1063/1.3050356

[Dynamics of the chain of forced oscillators with long-range interaction: From synchronization to chaos](#)

Chaos **17**, 043124 (2007); 10.1063/1.2819537

[Hyperlabyrinth chaos: From chaotic walks to spatiotemporal chaos](#)

Chaos **17**, 023110 (2007); 10.1063/1.2721237

[Complex dynamics in a nonlinear chemical system switching between two stable stationary states](#)

J. Chem. Phys. **119**, 3626 (2003); 10.1063/1.1592498



NEW Special Topic Sections

NOW ONLINE
Lithium Niobate Properties and Applications:
Reviews of Emerging Trends

AIP | Applied Physics
Reviews

Spatiotemporal chaos from bursting dynamics

Igal Berenstein and Yannick De Decker

Nonlinear Physical Chemistry Unit and Interdisciplinary Center for Nonlinear Phenomena and Complex Systems (CENOLI), Faculté des Sciences, Université libre de Bruxelles (ULB), Campus Plaine, C.P. 231, B-1050 Brussels, Belgium

(Received 19 May 2015; accepted 23 July 2015; published online 13 August 2015)

In this paper, we study the emergence of spatiotemporal chaos from mixed-mode oscillations, by using an extended Oregonator model. We show that bursting dynamics consisting of fast/slow mixed mode oscillations along a single attractor can lead to spatiotemporal chaotic dynamics, although the spatially homogeneous solution is itself non-chaotic. This behavior is observed far from the Hopf bifurcation and takes the form of a spatiotemporal intermittency where the system locally alternates between the fast and the slow phases of the mixed mode oscillations. We expect this form of spatiotemporal chaos to be generic for models in which one or several slow variables are coupled to activator-inhibitor type of oscillators. © 2015 AIP Publishing LLC. [<http://dx.doi.org/10.1063/1.4927911>]

I. INTRODUCTION

Because of the intrinsically nonlinear character of their kinetics, chemical reactions are often found to be at the heart of complex spatiotemporal dynamics. These behaviors can take different forms, including, for example, explosive transients accompanied by wave propagation or oscillations of the concentrations. The reaction-induced dynamical complexity culminates in the form of spatiotemporal chaos, in which the system is characterized by an apparent randomness of composition in both space and time. Spatiotemporal chaos has been observed experimentally and quantified on numerous occasions, including the Belousov-Zhabotinsky reaction in aqueous phase^{1,2} and redox reactions on surfaces.³⁻⁶

From a theoretical point of view, spatiotemporal chaos emerges from the equations that describe the evolution of the concentrations, which are usually of the reaction-diffusion type. Different mechanisms leading to such deterministic chaos have been identified. Generically speaking, chaotic behavior is observed as the consequence of successive qualitative changes of the dynamics (bifurcations). In homogeneous systems, the most common routes are period doubling of oscillatory processes,⁷ intermittency in which periodic behavior is interrupted by bursts of noise,⁸ and quasi-periodicity where the coexistence of two non-rational frequencies results in chaos.⁹ For inhomogeneous systems of large spatial extent, a comparable succession of transitions has also been observed,¹⁰ leading to a dynamics that is essentially unpredictable both in space and time. However, the different paths to spatiotemporal chaos have not been fully characterized yet.

On one hand, it has been observed in different models that having temporal chaos in the homogeneous limit is generally not sufficient to obtain spatially chaotic behaviors as well. There must also be a mechanism that breaks down the spatial homogeneity. Such mechanisms include point defects, i.e., locations in space where the system resides temporarily in a steady state, as is observed in the Willamowski-Rössler model.^{7,11} The breaking of spatial homogeneity can also appear

through line defects that correspond to lines of period 1 created by the collision of period 2 waves with shifted phases.¹⁰

On the other hand, it is also possible to generate spatiotemporal chaos when the homogeneous dynamics is itself non-chaotic. In such cases, the transport properties (diffusion, advection, etc.) play a central role. The Benjamin-Feir instability is a well known path to chaos in systems admitting a single limit cycle in the homogeneous limit.¹² A lack of efficient transport leads to a desynchronization of the oscillating behavior at different locations, generating phase instability and defect-mediated turbulence. Such turbulence has been observed, for example, in the two-variable Oregonator model, within the oscillatory regime.¹³ A similar behavior has been found in excitable systems, including the FitzHugh-Nagumo model.¹⁴ Spatiotemporal chaos can also be found when coupling together different non-chaotic spatiotemporal instabilities, like a Hopf and a Turing bifurcation.¹⁵ Another known path is spatiotemporal intermittency, where one observes an alternation between different attractors of the dynamical system, like in the Gray-Scott model.¹⁶⁻¹⁸

In this work, we show that spatiotemporal chaos can also emerge in the presence of *mixed-mode oscillations* of the bursting type, the homogeneous dynamics of which is non-chaotic. Mixed-mode oscillations consist in complex periodic behaviors in which fast oscillations are superimposed on slower ones, which results in multi-peaked variations of the concentrations. They are very common in chemistry: they have been observed in electrochemical reactions,^{19,20} in the peroxidase-oxidase reaction,^{21,22} and in the Belousov-Zhabotinsky reaction²³ to name but a few. Qualitatively speaking, they are known to arise because of the coexistence of fast and slow processes, which leads to dynamics with distinctly different time scales. Our main observation is that such separation of time scales can generate chaos in space through a mechanism that is different from the classical phase instability mentioned earlier. It is instead due to the inability of diffusion to “follow the pace” of fast oscillations. As a consequence, the system behaves as if there were two coexisting oscillators (a slow one and a fast

one), which leads to an effective intermittency where these behaviors alternate in space and time.

This idea is exemplified on an extension of a simple reaction-diffusion system known as the Oregonator model. We present this extended Oregonator in Section II, where we also detail the dynamical behavior of the system in the homogeneous limit. The spatiotemporal dynamics is presented and analyzed in Section III, in which a special emphasis is put on the properties of the observed spatiotemporal chaos and on the mechanism by which it emerges. In Section IV, we discuss the origin of the chaotic dynamics and the similarities between the mechanism by which it emerges and those put forth earlier in the literature, with a special emphasis on the generic bi-rhythmic model studied by Casagrande and Mikhailov.²⁴ Section V is devoted to the conclusions and to possible extensions of this work.

II. AN EXTENDED OREGONATOR MODEL

Our objective here is to devise a simple chemical model which is able to present mixed mode oscillations with two distinctly different time scales. Fast/slow oscillators can be constructed in a generic fashion by adding a slow variable to activator-inhibitor types of oscillating models.²⁵ In this work, we will consider the following extension of the two-variable Oregonator:

$$\dot{x} = \frac{1}{\varepsilon} \left[x(1-x) - f y \frac{x-q}{x+q} \right] + D_x \nabla^2 x, \quad (1)$$

$$\dot{y} = x - y - k_1 y + k_{-1} z + D_y \nabla^2 y, \quad (2)$$

$$\dot{z} = k_1 y - k_{-1} z + D_z \nabla^2 z, \quad (3)$$

where we do not note explicitly the time and space dependences, for clarity of presentation. The original model, comprising only the variables x and y , describes the spatiotemporal evolution of concentrations for the oscillating Belousov-Zhabotinsky chemical reaction.²⁶ Here, x represents the dimensionless concentration of an activator species X (standing for HBrO_2) and y that of an inhibitor Y (the oxidized version of the catalyst, ferriin). In the extension we proposed, Y is able to transform reversibly and slowly into an inactive form Z, whose dimensionless concentration is given by z . As mentioned above and showed in more detail below, this change will give rise to fast/slow oscillations. Similar features can be obtained by adding the same type of process to other activator-inhibitor schemes, like the Brusselator model. We decided to work here with the Oregonator because it opens the way to future experimental verification. We will discuss this point further in Sec. V.

The system of equations (1)-(3) admits up to three homogeneous steady states. One of them is trivial ($x = y = z = 0$) and linear stability analysis (see the Appendix for details) shows that it is always a saddle. There is in addition a pair of states characterized by $x_{\pm} = y_{\pm} = (k_{-1}/k_1) z_{\pm}$, with

$$x_{\pm} = \frac{1}{2}(1-q-f) \pm \frac{1}{2} \sqrt{1+q^2+f^2+2q-2f+6fq}. \quad (4)$$

In the limit of small ε , the state (x_-, y_-, z_-) is always a saddle, while the (x_+, y_+, z_+) solution can undergo two Hopf bifur-

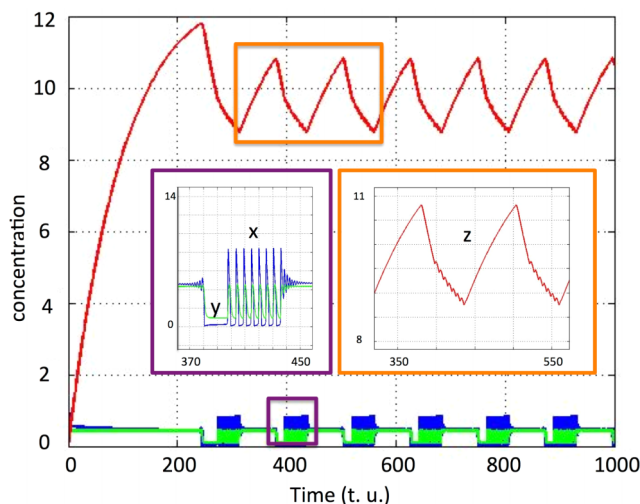


FIG. 1. Time series of concentrations (blue for x , green for y , and red for z), for a simulation of the homogeneous limit of models (1)-(3), using $\varepsilon = 0.04$, $q = 0.01$, $f = 0.6$, $k_1 = 0.3$, and $k_{-1} = 0.01$.

cations. For example, using k_1 as the control parameter, the stability analysis predicts two imaginary eigenvalues with a positive real part and one real negative eigenvalue for $0 < k_1 \leq k_1^{(1)}$ and $k_1 \geq k_1^{(2)}$, where $k_1^{(1)}$ and $k_1^{(2)}$ are intricate functions of the other parameters, the exact form of which is not relevant for our purpose. Consequently, temporal oscillations are to be expected in these regions of parameter space, as confirmed by numerical integration of the homogeneous system. The integrations additionally reveal that for $k_1 \leq k_1^{(1)}$, the oscillations can take the form of *mixed-mode oscillations*.

A typical example of such dynamical behavior is pictured in Fig. 1. After a relatively long induction period, the system displays series of fast oscillations (here, 8), followed by periods of latency during which x and y remain so to say constant, while z changes slowly. This type of mixed-mode oscillation is known as *bursting dynamics*. There exists a whole region in parameter space where such fast/slow mixed-mode oscillations can be observed. The number of fast oscillations per slow period changes in a stepwise fashion when varying the parameters, forming a “devil’s staircase” (see Fig. 2). Note that there are no windows of temporal chaos between the different steps.

This behavior differs remarkably from the dynamics displayed by the original two-variable Oregonator model, which for the same choice of parameters would generate simple (fast) oscillations. From a phase space perspective, the oscillations observed in the two-variable Oregonator correspond to a single-looped limit cycle emerging from a Hopf bifurcation. Our addition of a third dynamical variable results in a much more complex attractor in the three-dimensional phase space (see Fig. 3). It consists of a combination of a slow and a fast dynamics, with the latter having a number of windings that depends on the choice of parameters.

The trajectories in phase space and the corresponding oscillations can be understood qualitatively as follows. We note that the variable z oscillates slowly between two values all along the dynamics. It is thus relevant to consider an alternative dynamical system consisting of the homogeneous limit of

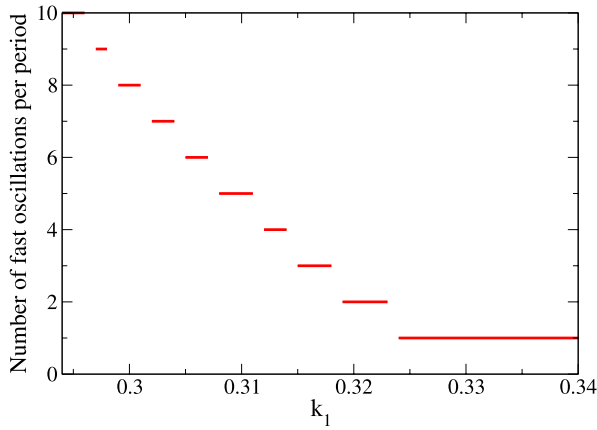


FIG. 2. Example of the “staircase” evolution of the number of fast oscillations per period in the asymptotic regime, obtained from the numerical integration of (1)-(3) with different values of k_1 (the other parameters being identical to those of Figure 1).

equations (1)-(3), but in which $z = z^*$ would be an externally controlled parameter,

$$\dot{x} = \frac{1}{\varepsilon} \left[x(1-x) - f y \frac{x-q}{x+q} \right], \tag{5}$$

$$\dot{y} = x - y - k_1 y + k_{-1} z^*. \tag{6}$$

This reduced system presents a supercritical Hopf bifurcation corresponding to a given value of $k_{-1} z^*$. An example of the corresponding bifurcation diagram is given in Fig. 4. We consider now a situation for which z^* would be controlled so to start from a rather low value and would then be increased and subsequently decreased, in order to mimic the large oscillations observed in the original system. At low values of $k_{-1} z^*$, the system is in a stable state, and as z^* increases, it crosses a saddle-node bifurcation bringing the system to a low value of x (and y). On the way back to low values of z^* , the system slowly crosses a Hopf bifurcation and reaches a limit cycle in the x, y plane corresponding to relatively large oscillations of these variables (see, again, Figure 4). The oscillations persist until $k_{-1} z^*$ reaches the lower bound of the domain of oscillations, at which point the trajectories become attracted to the original stable state and x and y do not oscillate anymore.

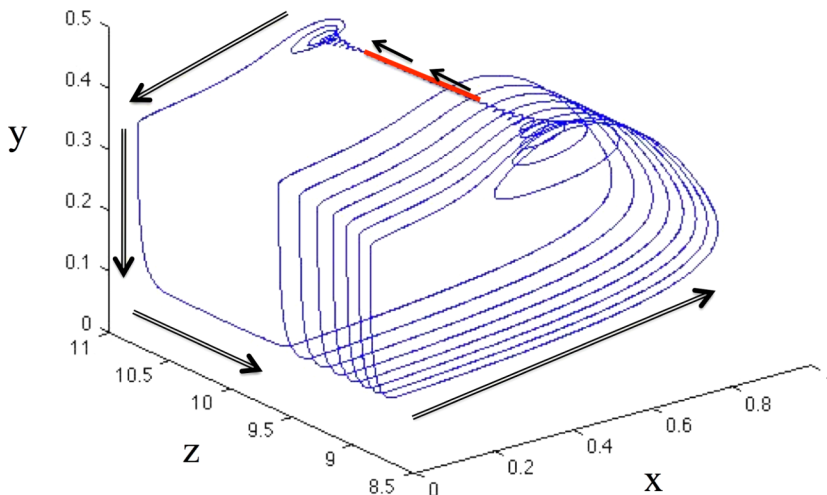


FIG. 3. Attractor in the x - y - z phase space, reconstructed from the time series in Fig. 1.

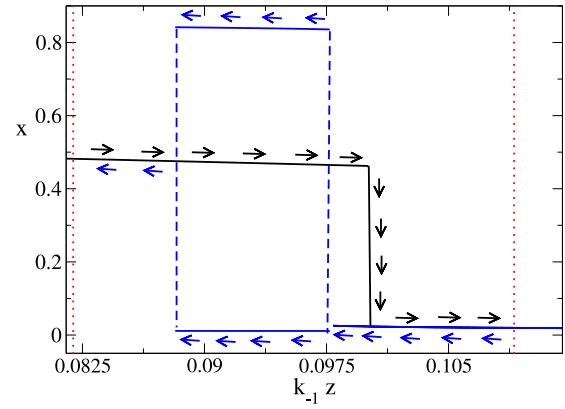


FIG. 4. Bifurcation diagram showing the extrema for the x variable, as obtained with numerical integration of the reduced system discussed in the text. The black line corresponds to the steady state obtained by increasing $k_{-1} z^*$, starting from low values, while the blue curves represent the asymptotic behavior on the way back from large to low values of this parameter. The values of the parameters are as in Figs. 1 and 2. The vertical red lines stand for the maximal and minimal values that $k_{-1} z^*$ takes during the oscillations, and the arrows indicate the increase and subsequent decrease of that variable.

The complex oscillations that we observe in the original model can be seen as a succession of such stages, as z slowly increases and decreases as a function of time. The exact time at which oscillations appear and the number of periods that is generated in the original model (1)-(3) depend on the ratio of time scales between the kinetics of z and that of the reduced system. In any case, and as long as the analogy with the simple 2-variable model holds, the behavior of the original 3-variable system can be understood as an effective “bistability” between a limit cycle and a stable point. This analogy, albeit qualitative by essence, will reveal important in understanding the origin of the spatiotemporal chaos that we describe in Sec. III.

III. SPATIOTEMPORAL DYNAMICS

We investigated the spatiotemporal dynamics of equations (1)-(3) numerically, with a finite-difference integration scheme for which the space and time steps were kept at $dl = 0.1$ and $dt = 1.0 \times 10^{-4}$. We first present the results obtained in a one dimensional system with no-flux boundary conditions and for

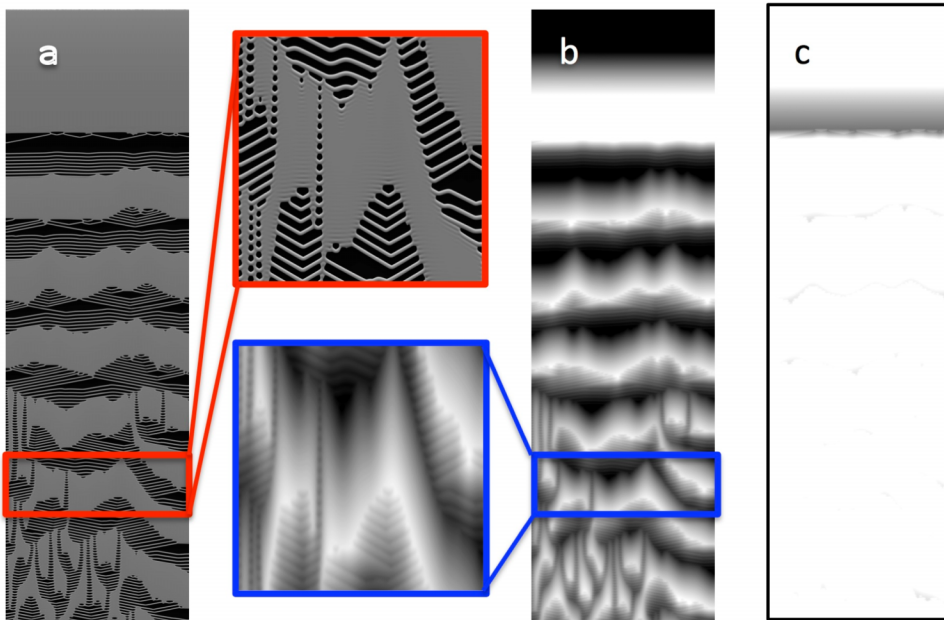


FIG. 5. Space-time plots for x (a) and z (b), with white (black) representing high (low) concentration. (c) plots the distance to the steady state, where black corresponds to a distance of 0. The size of the space-time plots is 100 space units (horizontal) by 1000 time units (vertical, increasing downwards), while the insets are 100×100 . Parameters are as in the previous figures, with $D_x = D_y = D_z = 0.1$. Random initial condition is used, with x and y ranging from 0 to 0.1 and z from 5 to 5.1.

identical mobilities of the three variables. Similar results were observed for other choices of the boundaries and diffusion coefficients (as long as they do not lead to a Turing instability). As can be seen in Fig. 5, the concentrations behave in a way that is very similar to the homogeneous limit *for short times*. We indeed recover the induction period, followed by the bursting dynamics. The number of bursts and the frequency of the oscillations are the same as those of the well-mixed case up to this stage. *For long enough times*, though, there is a marked transition to a much more turbulent regime, in which regions of fast and slow oscillations coexist in space.

The transition to the resulting spatiotemporal chaos occurs because, by the end of the induction periods, fast oscillations emerge from the quasi-stationary state preferentially at some locations in space and then propagate in a wave-like form. This propagation is characterized by an almost constant velocity, resulting in the v-shaped lines appearing in the space-time plots such as in Fig. 5(a). The collisions between waves seem to play an important role in the emergence of the turbulent behavior, as illustrated in Fig. 6 in which spatiotemporal maps are shown for different values of k_1 . We observe that spatiotemporal chaos does not develop when only fast oscillations

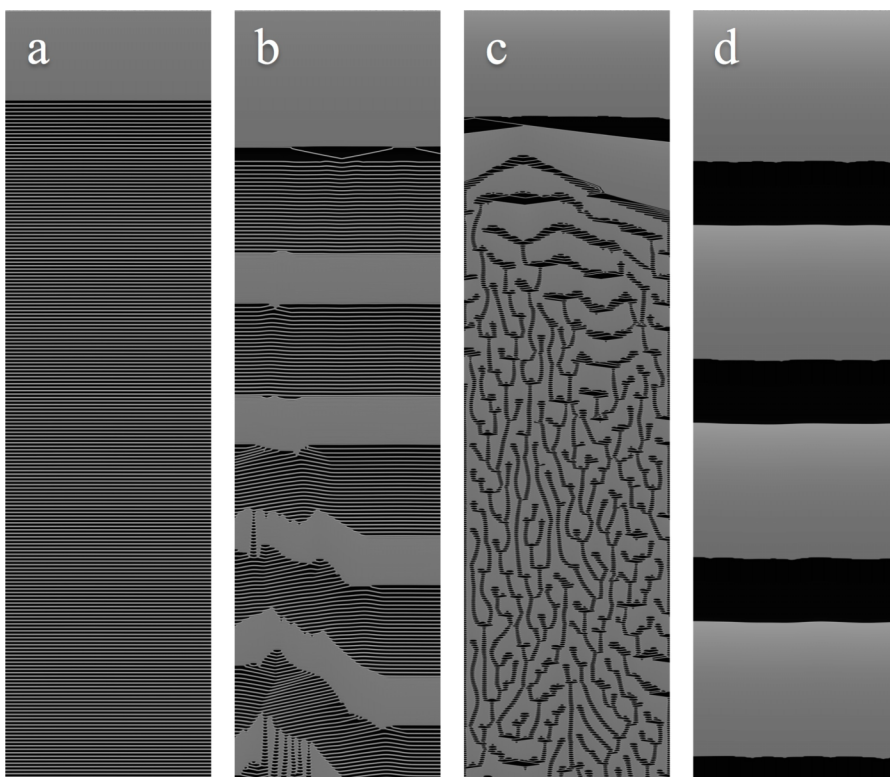


FIG. 6. Spatiotemporal maps showing the evolution of the variable x . The system is 100 space units wide (horizontal) and 1000 time units long (vertical) for (a) and (b) and 2000 time units long for (c) and (d). The parameters are the same as in Fig. 5, except for k_1 which is equal to 0.24 (a), 0.27 (b), 0.45 (c), and 0.8 (d), respectively.

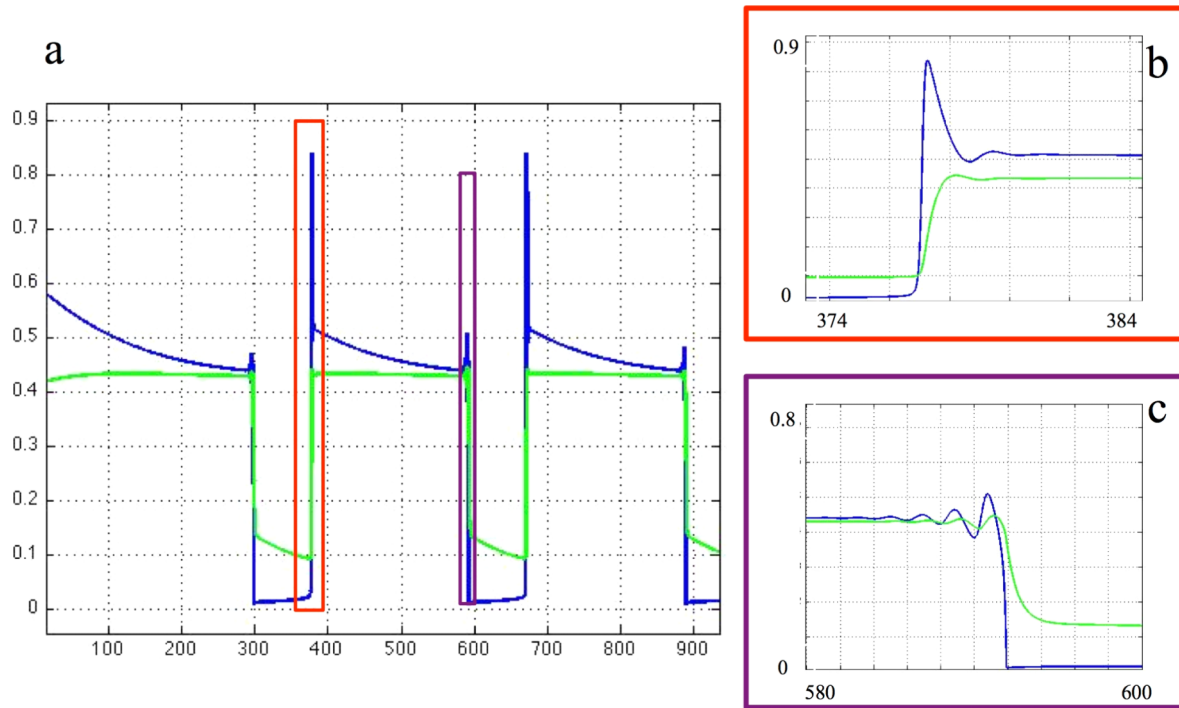


FIG. 7. Temporal evolution of the x (blue) and y (green) variables for $k_1 = 0.45$ (the other parameters remaining the same as before). The insets (b) and (c) show the rapid transient oscillations found during the early stage and the final stage of each cycle, respectively.

are present, i.e., for low values of k_1 (see Fig. 6(a)). Chaos appears as this parameter is increased and the system enters the regime of mixed-mode oscillations (Fig. 6(b)). It is also found for values of k_1 that correspond to single-mode slow oscillations (Fig. 6(c)), as long as these slow oscillations are accompanied by fast “internal” relaxations such as those depicted in Fig. 7. Spatiotemporal chaos disappears again (see Fig. 6(d)) for larger values of k_1 , for which the system presents simple slow oscillations without a fast relaxation stage. The coexistence of slow and fast dynamics thus seems to be a prerequisite for observing the kind of turbulence we report here.

We also investigated the development of spatiotemporal chaos in two dimensions. After a couple of bursting bulk oscillations, the system forms spiral waves at the tip of which there is a peak of concentration of Z (as seen in the central panels of Fig. 8). These peaks form over a period of time, which indicates that the tips do not move and therefore are not causing chaos by Doppler instability.²⁷ These spirals lose stability, and the alternation between a wave regime and a regime of quasi-stationary concentrations of X and Y begins. As can be seen in Fig. 8, a one-dimensional cut of the system presents features that are close to those of the one-dimensional simulations, with the propagation of waves of the rapidly oscillating transients.

IV. DISCUSSION

To what kind of spatiotemporal chaos do the above observations belong? In chaos due to phase instability, the lines of equal phase show no break.²⁸ For the system presented here, we observe islands of the phase of quasi-stationary concentrations of X and Y inside an oscillatory background, or the other way

around. This indicates a breakup of the phase, and therefore, what we observe is not such type of chaos. Defect-mediated turbulence is characterized by breaks in the phase, in which defects appear that correspond to a zero amplitude of the limit cycle. The local amplitude can be computed straightforwardly from simulations, since the coordinates of the unstable state inside the limit cycle are known analytically. We observe that the amplitude (in this case, the distance to the steady state) never reaches zero in the chaotic regime, as illustrated in Fig. 5(c). As a consequence, it cannot be said to be of the defect type either.

The fully developed spatiotemporal chaos we observe has instead characteristics that would correspond to an *effective intermittency*, by analogy with the behavior observed in several different reaction-diffusion systems.^{16,18,24,29} In the systems,^{16,18,29} the dynamics in the homogeneous limit shows three steady states, one that is stable, a saddle, and an unstable focus. This property reflects itself in the spatially extended case as chaotic transitions between a laminar phase, during which the system resides close to the stable steady state, and a turbulent phase, during which the system is in an oscillatory state. In the same spirit, Casagrande and Mikhailov²⁴ studied the dynamics generated by a Ginzburg-Landau equation coupled with a slow variable. They deduced that the homogeneous system is bi-rhythmic, i.e., that it admits two different oscillatory uniform states (one being slow and the second one being fast). They also observed through numerical simulations that bursts of the rapidly oscillating state in the slowly oscillating one can lead to a form of intermittent spatiotemporal chaos sharing strong similarities with our own observations (such as the wave-like propagation of the rapid oscillations). They attributed the origin of this behavior to a desynchronization of the two oscillators involved.

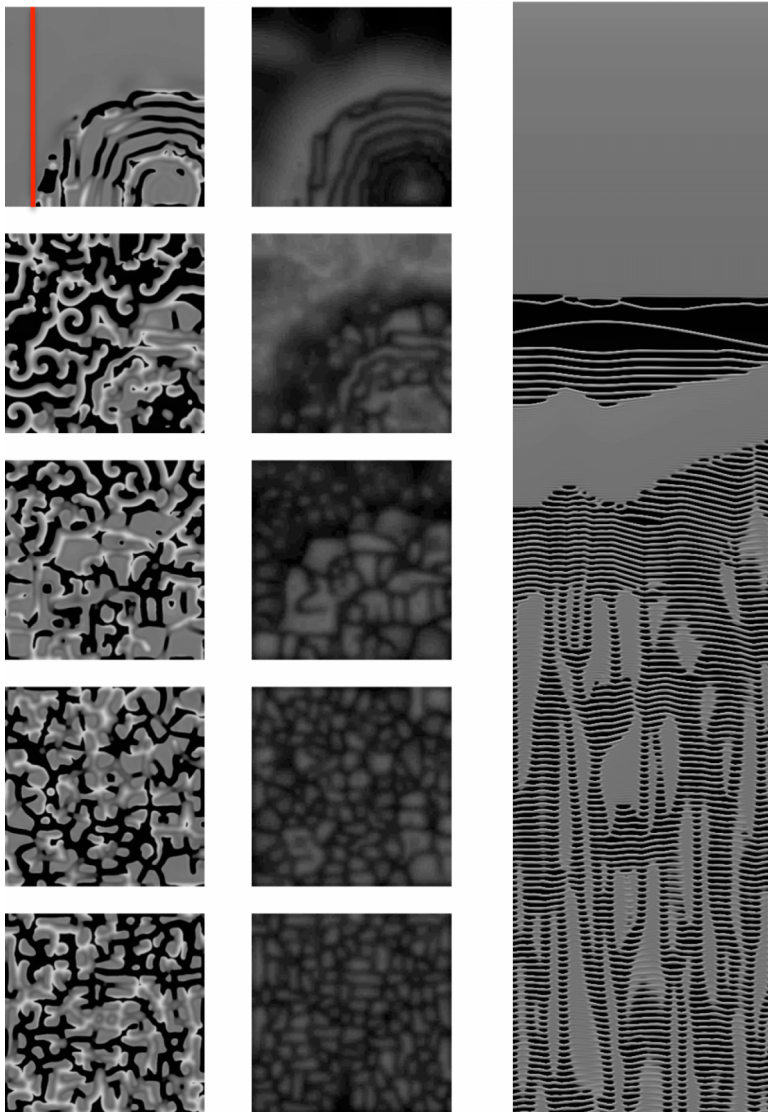


FIG. 8. Snapshots of patterns in x (left column) and z (center column). Each of these pictures corresponds to a size of 50×50 . The different snapshots were taken at times 60, 70, 80, 100, and 150, respectively. The rightmost column is a 1-dimensional space-time map corresponding to the red line in the first snapshot (total time = 150). The parameter values are identical to those of Fig. 5, except for $D_x = D_y = D_z = 0.05$. Initial conditions are as in Fig. 5.

The system we study only admits a single attractor in the homogeneous limit and a straightforward comparison with the above studies is not possible. However, its dynamics can qualitatively be seen as an alternation between a limit cycle and a stable state for the x and y variables, with the alternation being made possible because z itself oscillates slowly between two extremal values, as discussed in Section II. In this sense, we could say that the spatiotemporal chaos that we observe finds its origins in an “effective bi-rhythmicity.” One oscillatory state would correspond to slow and ample variations of z during which x and y would remain almost constant, which would be similar to the laminar phases of the studies mentioned above. The other oscillation would correspond to rapid oscillations of all the variables, with a large amplitude for X and Y and a small one for Z . The complex dynamics that we are facing could thus be seen as effective intermittency involving two “pseudo-attractors,” the coexistence of which resides in the separation of time scales that is characteristic of mixed mode oscillations. This intermittent-like behavior is further confirmed by the fact that the probability $P(T)$ for the system to reside for a time T in the fast stage of the oscillations follows like most intermittent systems a power law distribution of the form $P(T) \propto T^{-\gamma}$, with

$\gamma = 1.0 \pm 0.3$ (see Fig. 9). We insist however on the fact that the system we study is only qualitatively amenable to the above mentioned works, since it involves a single limit cycle and since the chaotic behavior is observed only far from the Hopf bifurcation point in the region of bursting oscillations. When k_1 is close to the Hopf line, only slow and regular bulk oscillations comparable to those shown in Fig. 6(d) are found. When varying other parameters, complex oscillations can be found even close to the Hopf bifurcation, but chaos was never observed.

The mechanism leading to such fully developed spatiotemporal chaos in our case seems to stem from a combination of sensitivity to initial conditions and lack of synchronization. We see indeed in Figs. 5 and 8 that the number of fast oscillations between slow oscillations actually varies from one point to another. These differences can be qualitatively explained by the intricate shape of the underlying local attractor and by the complex trajectories leading to it. Consider again the case of a homogeneous system, whose phase space is three dimensional. For our choice of parameters, any initial condition will, for long enough times, lead to trajectories in that space as pictured in Fig. 3. Our numerical investigations

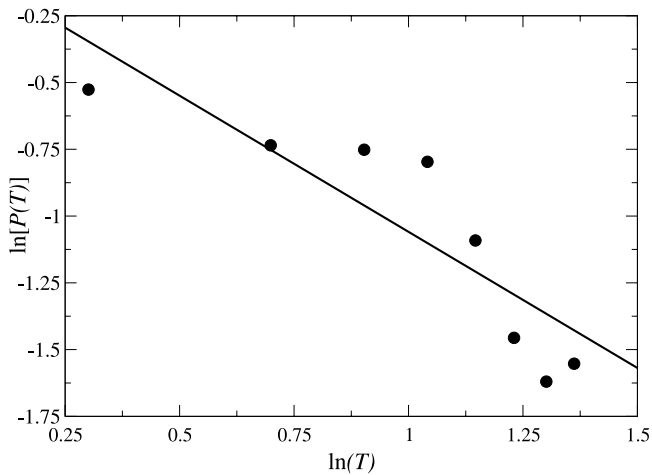


FIG. 9. Log-log plot of the probability $P(T)$ for the system to reside for a time T in the fast stage of the oscillations. The straight line represents the best linear fit, whose slope is equal to $-(1.0 \pm 0.3)$. The statistics were obtained from numerical simulations of a one-dimensional system with parameter values identical to those of Fig. 5, except for $k_1 = 0.26$. The size of the system was 100 space units and the statistics were performed over 1000 time units in the asymptotic regime.

however revealed that the properties of the transients towards such attractor are extremely sensitive to the choice of initial conditions. Two nearby points lead to transients having a different number of windings in phase space. The number of fast oscillations included in the transient dynamics changes consequently. Because of this, regions of almost constant x and y concentrations will coexist with regions of rapid oscillations in the case of spatially extended systems.

The initial conditions used in numerical integrations are such that the different points in space start from different locations in phase space, which explains why the fast oscillations start at different times and present a different number of windings. Transport by diffusion plays a central role in this regard. If the points in space were uncoupled, the different locations would give rise to unsynchronized dynamics evolving in parallel. Transport by diffusion should in principle smooth out these differences, but in the case hereby considered, it cannot ensure homogenization because, again, of the separation of time scales. For our choice of parameters, transport by diffusion is so much slower than the fast oscillations that it will “feel” only the average concentrations of the different species during these rapid transients. As these averages are extremely close to the almost stationary values of the slow part of the dynamics, the effective gradients of concentration are weak and the diffusion flux is very low. Diffusion is in some way blind to the different stages of the complex oscillations and hence unable to ensure synchronization. Local initial conditions and diffusion thus make for effective “fluctuations” that are not washed out, which results in unsynchronized local behaviors and, ultimately, in spatiotemporal chaos in the form of an effective intermittency.

V. CONCLUSIONS

To summarize, we have shown a new way for generating spatiotemporal chaos in systems whose homogeneous dy-

namics is non-chaotic, but consists instead in fast/slow mixed-mode oscillations characterized by a unique limit cycle. We exemplified this path to chaos on a simple extension of the Oregonator model, but we expect this mechanism to be generic, as we have tested a similar extension in other simple oscillating models (such as the Brusselator) and obtained again spatiotemporal chaos with similar characteristics. The origin of the spatiotemporal chaotic behavior resides in a desynchronization between regions that are in the rapidly oscillating phase of the mixed-mode oscillation and regions that are in its slow part. The resulting fully developed chaos consequently consists in a form of intermittency where the system locally alternates between the fast and slow phases in an irregular fashion. This behavior takes place far from the Hopf bifurcation, contrary to other known forms of spatiotemporal chaos.^{13,14,18,24}

It would be highly desirable to rationalize the genericity of this path to chaos in terms of the properties of the underlying phase space dynamics. The role played by the separation of time scales can indeed be formalized, in principle, by decomposing the dynamics more rigorously into a reduced and a layer problem, so that a critical manifold be defined. For the example we consider here, this manifold depends in a rather complex way on the coordinates (x, y, z) and this approach does not really help to rationalize our observations. It would be relevant to perform such a detailed, analytical study on simpler models, like an extended Brusselator.

Our choice of model was motivated by the potentiality of an experimental verification. The experimental study of spatiotemporal dynamics with mixed-mode oscillation is quite recent. The Belousov-Zhabotinsky reaction shows the formation of period 2 and period 3 spiral waves, together with line defects.^{10,30} The oscillations are not of the bursting type, so we do not expect the type of spatiotemporal chaos we identified here to show up in such experiments. However, it could be obtained in a version of the Belousov-Zhabotinsky reaction, in which a metal catalyst in its oxidized form would bind reversibly to a gel matrix, as has been done for oscillations in viscosity coupled to chemical oscillations.^{31,32}

ACKNOWLEDGMENTS

I.B. thanks the Bureau des Relations Internationales et de la Coopération of the ULB for the financial support.

APPENDIX: LINEAR STABILITY ANALYSIS

In this section, we provide details on the linear stability analysis of the homogeneous steady states corresponding to the set of equations (1)-(3). The Jacobian matrix for this system reads

$$\mathcal{J} = \begin{pmatrix} \frac{1 - 2\bar{x} - \frac{2f\bar{x}q}{(\bar{x}+q)^2}}{\varepsilon} & \frac{f(q - \bar{x})}{\varepsilon(q + \bar{x})} & 0 \\ 1 & -1 - k_1 & k_{-1} \\ 0 & k_1 & -k_{-1} \end{pmatrix}, \quad (\text{A1})$$

in which \bar{x} stands for the steady state value of that variable.

The eigenvalues of the linear stability analysis are found by solving the following cubic equation:

$$\omega^3 - \mathcal{A}\omega^2 + \mathcal{B}\omega - C, \quad (\text{A2})$$

where \mathcal{A} is the trace of \mathcal{J} , \mathcal{B} the sum of its principal minors, and C its determinant. One can thus have either three real eigenvalues or one real eigenvalue and two complex conjugates.

For state $(0, 0, 0)$, the determinant $C = k_{-1}(f + 1)/\varepsilon$ is always positive and so is thus the product of the eigenvalues. This state is consequently always unstable. The other coefficients read

$$\mathcal{A} = \frac{1}{\varepsilon} - (k_1 + k_{-1} + 1), \quad (\text{A3})$$

$$\mathcal{B} = k_{-1} - \frac{f + 1 + k_1 + k_{-1}}{\varepsilon}. \quad (\text{A4})$$

By Descartes' rule of signs, for polynomial (A2) to have up to 3 real positive roots, one needs to have at the same time $\mathcal{A} \geq 0$ and $\mathcal{B} \geq 0$. The first condition implies that $(k_1 + k_{-1} + 1)/\varepsilon \geq (k_1 + k_{-1} + 1)^2$ and one reaches the conclusion that under this condition, $\mathcal{B} \leq 0$ so that at least one of the eigenvalues is negative. Since moreover the two conditions for a Hopf bifurcation $\mathcal{A}\mathcal{B} - C = 0$ and $\mathcal{B} > 0$ cannot be satisfied simultaneously, one concludes that this steady state is characterized by one real positive and 2 real negative eigenvalues and is thus a saddle.

The case of the states (x_-, y_-, z_-) and (x_+, y_+, z_+) is much less straightforward as the signs of the different coefficients depend on the nature of the steady state as well as on the values of the different parameters involved. One can show however numerically that for $\varepsilon \ll 1$, the state (x_-, y_-, z_-) admits two real negative and one real positive eigenvalues. The other steady state always has one real negative eigenvalue but the two other ones can be imaginary for an appropriate choice of parameters. As mentioned in the text, keeping all the other parameters constant, the real part of these eigenvalues crosses zero for two distinct values of k_1 , $k_1^{(1)}$, and $k_1^{(2)}$ with $k_1^{(1)} \leq k_1^{(2)}$, which thus correspond to Hopf bifurcations. As an example, for the

set of parameters used in the manuscript, one has $k_1^{(1)} \approx 1.969$ and $k_1^{(2)} \approx 3.811$. The steady state (x_+, y_+, z_+) corresponds to a stable focus-node for values of k_1 comprised between these two limits and is a saddle-focus otherwise.

- ¹Q. Ouyang and J.-M. Flesselles, *Nature* **379**, 143 (1996).
- ²C. Qiao, H. Wang, and Q. Ouyang, *Phys. Rev. E* **79**, 016212 (2009).
- ³S. Jakubith, H. H. Rotermund, W. Engel, A. von Oertzen, and G. Ertl, *Phys. Rev. Lett.* **65**, 3013 (1990).
- ⁴M. Kim, M. Bertram, M. Pollmann, A. von Oertzen, A. S. Mikhailov, H. H. Rotermund, and G. Ertl, *Science* **292**, 1357 (2001).
- ⁵C. Beta, A. S. Mikhailov, H. H. Rotermund, and G. Ertl, *Europhys. Lett.* **75**, 868 (2006).
- ⁶D. Krefling and C. Beta, *Phys. Rev. E* **81**, 036209 (2010).
- ⁷A. Goryachev and R. Kapral, *Phys. Rev. Lett.* **76**, 1619 (1996).
- ⁸H. L. Swinney, *Phys. D* **7**, 3-15 (1983).
- ⁹L. Györgyi and R. J. Field, *Nature* **355**, 808 (1992).
- ¹⁰J. S. Park, S. J. Woo, O. Kwon, T. Y. Kim, and K. J. Lee, *Phys. Rev. Lett.* **100**, 068302 (2008).
- ¹¹J. Davidsen and R. Kapral, *Phys. Rev. Lett.* **91**, 058303 (2003).
- ¹²P. Couillet, L. Gil, and J. Lega, *Phys. Rev. Lett.* **62**, 1619 (1989).
- ¹³I. Berenstein and C. Beta, *J. Chem. Phys.* **135**, 164901 (2011).
- ¹⁴C. Zhang, H. Zhang, Q. Ouyang, B. Hu, and G. H. Gunaratne, *Phys. Rev. E* **68**, 036202 (2003).
- ¹⁵A. De Wit, G. Dewel, and P. Borckmans, *Phys. Rev. E* **48**, R4191 (1993).
- ¹⁶J. H. Merkin, V. Petrov, S. K. Scott, and K. Showalter, *Phys. Rev. Lett.* **76**, 546 (1996).
- ¹⁷I. Berenstein and Y. De Decker, *Chaos* **24**, 043109 (2014).
- ¹⁸R. Wackerbauer and K. Showalter, *Phys. Rev. Lett.* **91**, 174103 (2003).
- ¹⁹F. N. Albahadily, J. Ringland, and M. Schell, *J. Chem. Phys.* **90**, 813 (1989).
- ²⁰T. G. J. van Venrooij and M. T. M. Koper, *Electrochim. Acta* **40**, 1689 (1995).
- ²¹T. Hauck and F. W. Schneider, *J. Phys. Chem.* **97**, 391 (1993).
- ²²M. J. B. Hauser and L. F. Olsen, *J. Chem. Soc., Faraday Trans.* **92**, 2857 (1996).
- ²³D. Barkley, *J. Chem. Phys.* **89**, 5547 (1988).
- ²⁴V. Casagrande and A. S. Mikhailov, *Phys. D* **205**, 154 (2005).
- ²⁵J. Honerkamp, G. Mutschler, and S. Reitz, *Bull. Math. Biol.* **47**, 21 (1985).
- ²⁶J. J. Tyson and P. C. Fife, *J. Chem. Phys.* **73**, 2224 (1980).
- ²⁷L. Q. Zhou and Q. Ouyang, *J. Phys. Chem. A* **105**, 112-118 (2003).
- ²⁸B. I. Shraiman, A. Pumir, W. Van Saarloos, P. C. Hohenberg, H. Chaté, and M. Holen, *Phys. D* **57**, 241-248 (1992).
- ²⁹M. Argentina and P. Couillet, *Phys. A* **257**, 45-60 (1998).
- ³⁰J. S. Park and K. J. Lee, *Phys. Rev. Lett.* **83**, 5393 (1999).
- ³¹Y. Hara and R. Yoshida, *J. Chem. Phys.* **128**, 224904 (2008).
- ³²D. Suzuki, H. Taniguchi, and R. Yoshida, *J. Am. Chem. Soc.* **131**, 12058-12059 (2009).